An Effective and Efficient Approach to 3D Reconstruction and Quantification of Brain Tumor on Magnetic Resonance Images

Megha P. Arakeri and G. Ram Mohana Reddy

National Institute of Technology Karnataka (NITK), Surathkal, India
meghalakshman@gmail.com

Abstract

Three dimensional (3D) reconstruction of the tumor from medical images is an important operation in the medical field as it helps the radiologist in the diagnosis, surgical planning and biological research. Thus in this paper, we propose an effective and efficient approach to 3D reconstruction of brain tumor and estimation of its volume from a set of two dimensional (2D) cross sectional magnetic resonance (MR) images of the brain. In the first step, MR images are preprocessed to improve the quality of the image. Next, abnormal slices are identified based on histogram analysis and tumor on those slices is segmented using modified fuzzy c-means (MFCM) clustering algorithm. Next, the proposed enhanced shape based interpolation technique is applied to estimate the missing slices accurately and efficiently. Then, the surface mesh of the tumor is reconstructed by applying the marching cubes (MC) algorithm on a set of abnormal slices. The large number of triangles generated by the MC algorithm was reduced by our proposed mesh simplification algorithm to accelerate the rendering phase. Finally, rendering was performed by applying Phong lighting and shading model on the reconstructed mesh to add realism to the 3D model of the tumor. The volume of the tumor was also computed to assist the radiologist in estimating the stage of the cancer. All experiments were carried out on MR image datasets of brain tumor patients and satisfactory results were achieved. Thus, our proposed method can be incorporated into the computer aided diagnosis (CAD) system to assist the radiologist in finding the tumor location, volume and 3D information.

Keywords: *Brain tumor, Magnetic resonance imaging, 3D reconstruction, Interpolation, Mesh simplification*

1. Introduction

Brain tumor is inherently serious and life-threatening because of its invasive and infiltrative character in the limited space of the intracranial cavity. Hence determining its pathology, volume and complexities is crucial for surgical planning and knowing the stage of cancer. Magnetic resonance imaging (MRI) is the commonly used imaging modality for non-invasive analysis of the brain tumor. MRI uses radio waves and magnetic fields to acquire a set of cross sectional images of the brain. That is anatomic details of the 3D tumor are presented as a set of 2D parallel cross sectional images. Representation of a 3D data in the form of 2D projected slices does result in loss of information and may lead to erroneous interpretation of results [1]. Also, 2D images cannot accurately convey the complexities of human anatomy and hence interpretation of complex anatomy in 2D images requires special training. Although radiologists are trained to interpret these images, they often find difficulty in communicating their interpretations to a physician, who may have difficulty in imagining the 3D anatomy. Hence, there is a need for 3D reconstruction of the tumor from a set of 2D parallel cross

sectional images of the tumor. 3D visualization enables better understanding of the topology and shape of the tumor, and enables measurements of its geometrical characteristics. The extracted information is helpful in staging of tumor, surgical planning, and biological research [2]. Therefore, how to reconstruct a trustworthy surface from the sequential parallel 2D cross sections becomes a crucial issue in biomedical 3D visualization.

2. Proposed Methodology

The main task of 3D reconstruction of the tumor from a set of 2D parallel cross sectional images is divided into several subtasks as shown in Figure 1.

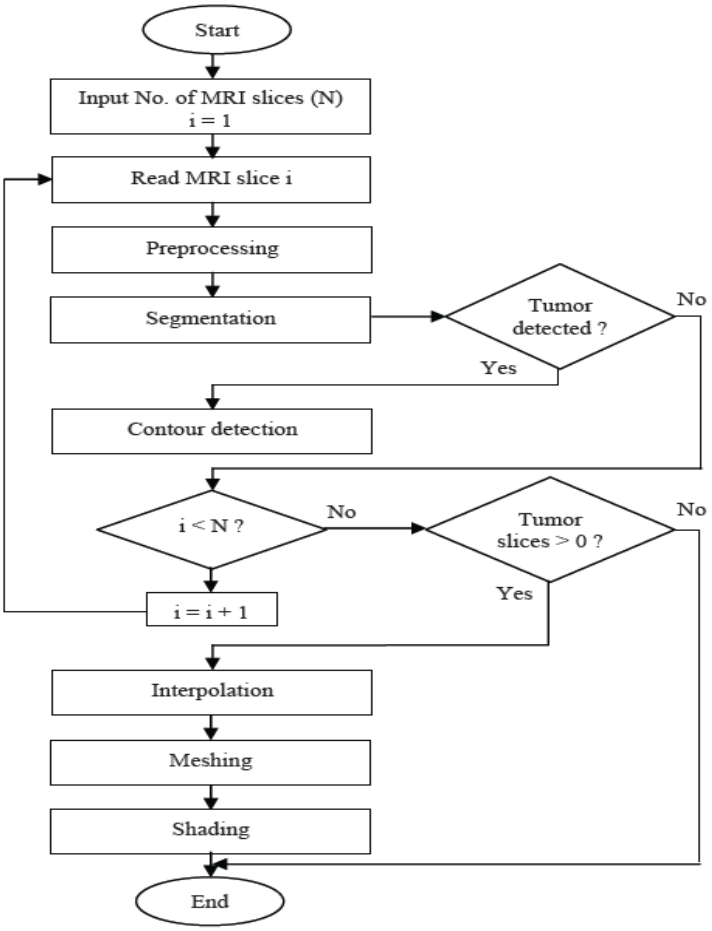

Figure 1. Flowchart of the Proposed 3D Tumor Reconstruction Approach

In the first step, preprocessing is performed to improve the quality of the acquired images. Then the segmentation is performed by modified fuzzy c-means (MFCM) clustering algorithm [8] on each abnormal slice of the brain to identify the region of the tumor. The normal slices are eliminated from the set. In order to provide the smooth surface, the gap between the slices is filled by performing inter-slice interpolation using the proposed enhanced shape based interpolation technique. In the next step, slices are connected through a triangulation to generate mesh of the tumor in 3D space using the

marching cubes (MC) algorithm [4]. The large number of triangles in the surface mesh is reduced by the proposed mesh simplification algorithm. The realistic effects are added to the tumor by shading the generated mesh. Finally, the volume of the tumor is computed from the abnormal slices.

2.1. Preprocessing

The noise can mask and blur the important features in the MR image and thus make the further steps in medical image analysis difficult. In this work, the noise has been eliminated from MR images by applying 3×3 median filter resulting in the smoothening of edges in the image. Hence, to improve the perceptibility of the tumor and other structures in the brain unsharp masking was used after median filtering. A 3×3 unsharp filter was constructed using the negative of the 2D Laplacian filter. The sizes of filters were chosen empirically. Image contrast was enhanced by applying histogram equalization. As the analysis has to be performed on brain region, the skull region was eliminated from each MR image of the brain by converting original MR image to a binary image and retaining only the pixels in the largest connected component which corresponds to the brain region.

2.2. Segmentation

MRI of the brain gives a set of slices containing normal and abnormal slices. Hence, before segmentation we need to identify the abnormal slices containing the tumor. The normal slice consists of three regions white matter (WM), gray matter (GM) and cerebrospinal fluid (CSF). Whereas a slice with tumor consists of four regions (WM, GM, CSF and tumor). Thus in order to determine whether the given MR image of the brain is normal or abnormal, the histogram of the brain region is computed using Equation (1) and the number of clusters present in the brain region is determined based on the histogram analysis [7].

$$h(g) = \frac{\sum_{x=0}^{M-1}\sum_{y=0}^{N-1}\delta(I(x,y)-g)}{M \times N} \tag{1}$$

Where, the function $h(g)$ gives the number of pixels having a gray level equal to g in the image of size $M \times N$. The gray level g lies in the range $[0:L-1]$ and L is the maximum gray level in the image. Function $\delta(0) = 1$ and $\delta(g \neq 0) = 0$. If the histogram consists of three peaks then the given MR image is considered as the normal slice and further processing of the MR image is not carried out. Otherwise, we consider that the slice contains the abnormal region and proceed to apply our previously proposed brain tumor segmentation method [8] which combines wavelet transform and MFCM clustering algorithm to segment the tumor in the MR image. The resulting clusters of the brain region are shown in Figure 2. The contour of the tumor is identified using 4-connected neighbors.

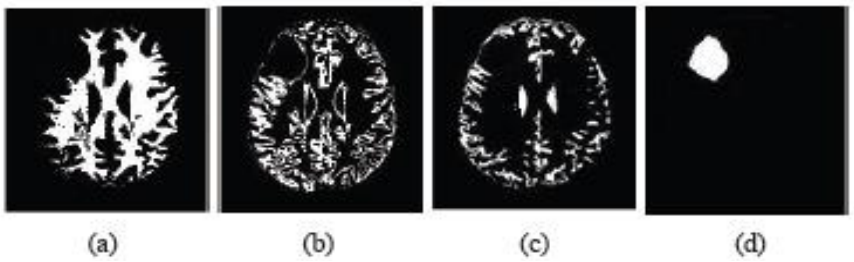

Figure 2. Clusters of the Brain in MR Image: (a) White Matter (b) Gray Matter (c) Cerebrospinal Fluid (d) Tumor

2.3. Inter-Slice Interpolation

After the segmentation, slices of the segmented tumor are stacked up to form the volume data in the 3D space. Generally, the set of slices acquired from the MRI device is such that the distance between the slices is larger than the distance between the pixels within the slice. The surface reconstructed with such a set of slices is inaccurate and not smooth. Thus in this work, the missing slices are estimated using our proposed enhanced shape based interpolation technique. The original shape based interpolation proposed by Raya *et al.*, [3] converts binary image into a gray scale image via a city block distance transform which assigns to every point in the binary image a gray level equal to its shortest distance from the boundary of the object. Then the intermediate slice is estimated by linearly interpolating the distances on two sequential slices. Finally, the interpolated image is converted to a binary image by threhsolding at zero. The Euclidian distance transform is a global operation since for each pixel a shortest distance to boundary pixel must be assigned. Therefore it requires $O(n^2)$ operations. Hence, the city block distance transform which computes the distance transform based on n-neighborhood was used in the original shape based interpolation. However, the city block distance metric provides faster computation of the distance transform but it provides a bad approximation to the Euclidian distance [9]. This is because, the city block distance metric over estimates the diagonal distances since it counts diagonal connections as 2 steps, rather than $\sqrt{2}$. Thus in the present work, another n-neighborhood distance metric called chamfer distance metric used by Herman *et al.*, [10] is incorporated to perform distance transform in shape based interpolation. It counts the horizontal/vertical connections as 1 and diagonal connections as $\sqrt{2}$ Hence, it better approximates the Euclidean distance compared to the city block distance metric. Since the distance transform is computed by considering the local neighborhood, it requires only $O(n)$ operations and thus consumes less time compared to the Euclidean distance transform [11].

Another problem with shape based interpolation is that it produces anomalous results if there is a drastic shift in the object position on sequential slices. That is the object reconstructed with such a set of slices is not accurate. In order to overcome this problem we perform centroid alignment of the tumors to match the centroids of tumors in the consecutive slices prior to interpolation. This results in gradual changes in both shapes and spatial positions of the object in interpolated slices. With the above two concepts incorporated into the original shape based interpolation algorithm, we summarize our enhanced shape based interpolation algorithm as follows:

Algorithm 1: Slice_Interpolation
Input: Two consecutive slices of the scanned tumor.
Output: original and estimated slices.

Begin

1. Compute the centroid *(C)* of the consecutive slices *a* and *b*.
2. Compute the centroids C_s and C_t of the tumor region R_s and R_t on slice *a* and *b* respectively.
3. Translate R_s and R_t to align the centroids C_s and C_t on the line passing through the centroids of the slices.
4. Perform shape based interpolation.

   4.1. Compute a distance transform for slice *a* and *b*.

$$D(x,y,z)=\begin{cases}0 \quad ,(x,y,z)\in bO\\ +d(x,y,z), \quad (x,y,z)\in O\setminus bO.\\ -d(x,y,z), \quad (x,y,z)\notin O.\end{cases}$$

   Where, *O* represents the tumor region R_s or R_t and *bO* represents the boundary of the tumor region on slice *z = a,b*. *d(x,y,z)* represents chamfer DT of point *(x,y,z).*

   4.2. Interpolate distance values on slice *a* and *b* using linear interpolation to determine pixel value on new slice z.

$$D(x,y,z)=D(x,y,a)+\frac{z-a}{b-a}(D(x,y,b)-D(x,y,a))$$

   4.3. Convert the gray scale image to binary image.
5. Restore R_s and R_t to its original position.
6. Compute the new centroid for a newly interpolated slice.

$$C_z=C_S+\frac{z-a}{b-a}(C_T-C_S)$$

7. Translate the tumor region R_z on new cross section to a new location using the corresponding centroid C_z.

End.

2.4. Mesh Generation

Once we have the complete set of slices, we apply the MC algorithm proposed by Lorensen *et al.*, [4] to reconstruct 3D surface of the tumor from a set of 2D cross sectional images. The MC algorithm operates on a logical cube created from eight pixels; four each of two adjacent slices. It processes one cube at a time and determines how the surface intersects each cube using the isovalue of the surface and cube-isosurface intersection patterns shown in Figure 3. The problem with these patterns is that there is a possibility of ambiguous faces and hence holes to appear in the reconstructed surface. An ambiguous face is the one which has an intersection point in each of its four edges. In this case, the topologically correct connection between the intersection points becomes ambiguous, which leads to the hole problem with MC [12].

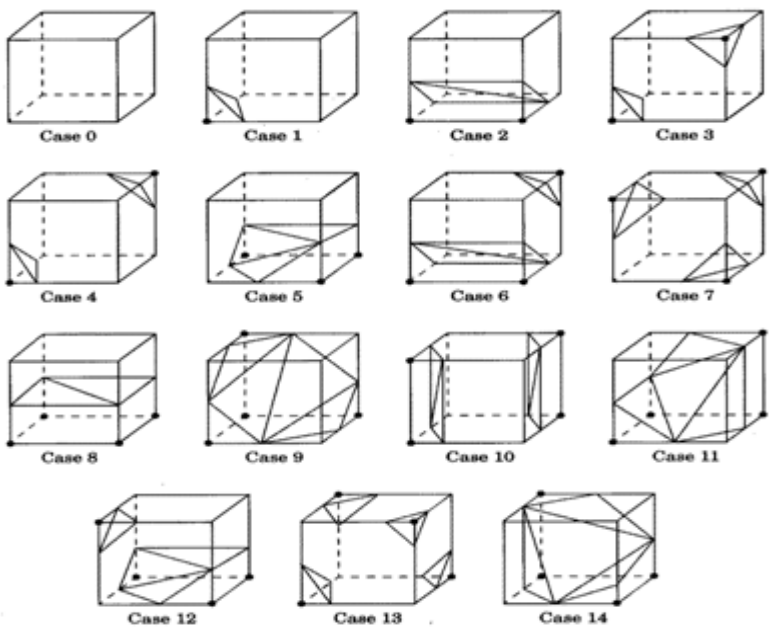

Figure 3. Basic Cube-Isosurface Intersection Patterns

It was observed that only patterns 3, 6, 7, 10, 12 and 13 have ambiguous face and hence modification was required only for these patterns. In order to solve the hole problem in these patterns, we employed the method developed by Montani et al. [13]. By this method, the additional six patterns shown in Figure 4 which are complement of patterns 3, 6, 7, 10, 12, 13 were added to the list of basic 15 patterns. Thus, we considered total 21 patterns to identify cube-surface intersection in the process of surface reconstruction of the tumor. With the help of intersection points and cube-isosurface intersection patterns the mesh of triangles was generated to represent the 3D surface of the tumor.

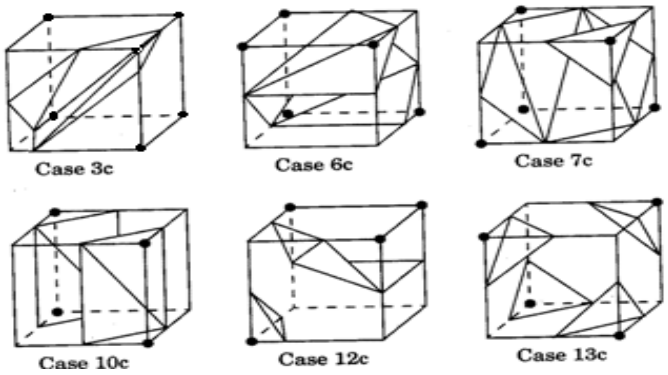

Figure 4. Cube Configurations to Solve the Ambiguity Problem [13]

2.5. Mesh Simplification

The MC algorithm results in a large number of triangles. Hence, we propose a mesh simplification algorithm for accelerating the rendering phase and saving storage space. Among the existing mesh simplification algorithms, Qslim [5] and memoryless simplification (MS) [6] are identified as best algorithms with respect to producing high

quality simplified mesh models. But both of these algorithms cannot preserve important shape features such as highly curved regions as their error metrics is based on distance metric and volume loss, respectively. In order to overcome these drawbacks we propose a mesh simplification method where edges are iteratively collapsed based on the error metric consisting of curvature, volume loss and shape of adjacent triangles. The curvature factor helps in identifying flat and curved regions in the mesh. Thus with the help of vertex curvature, mesh simplification can be performed in flat regions and thus preserving details of highly curved region. Whereas volume loss and shape of adjacent triangles help in preserving the shape of the original model and avoid skinny triangles which do not contribute much to mesh geometry.

The notations used in the proposed mesh simplification method are shown in Table 1. The proposed method has a two phase greedy approach to mesh simplification where edge collapsing is performed iteratively by collapsing in each step least significant edge of internal vertices on a flat region of the mesh.

Table 1. Notations for Mesh Simplification Algorithm

Symbol	Description
v_i	Vertex of mesh M
e_{ij}	Edge of mesh M connecting set of vertices $\{v_i, v_j\}$. v_i and v_j form origin and head of e_{ij}.
t	Triangular face of M is a set of edges (e_{ij}, e_{jk}, e_{ki}) or vertices (v_i, v_j, v_k)
T_{v_i}	Set of triangles incident on vertex v_i
$T_{e_{ij}}$	Set of triangles incident on edge $e_{ij.}$
E_{v_i}	Set of edges incident on vertex v_i
N_{v_i}	Set of vertices in the neighborhood of vertex v_i

During the edge collapse the start point is removed and the position of the end point is taken as the position of the new vertex. Removing boundary vertices may distort the shape of the mesh and hence edge collapse operation is performed on internal vertices. Details of the two phases of the proposed mesh simplification are given below.

- **Phase-I: Assignment of Vertex Priority**

In this phase, interior vertices of the mesh are prioritized based on curvature at a vertex. This is because the aim is to collapse more edges in flat regions and retain details of highly curved regions. The curvedness R at a vertex is defined by using mean curvature and Gaussian curvature as given below [14].

$$R = \sqrt{2H^2 - K} \tag{2}$$

Where, H and K represent mean curvature and Gaussian curvature at a vertex respectively. They are defined by the following equations.

$$K = \frac{2\pi - \sum_{i=1}^{n} \alpha_i}{\frac{1}{3}A} \qquad H = \frac{\frac{1}{4}\sum_{i=1}^{n} \| e_i \| \beta_i}{\frac{1}{3}A} \tag{3}$$

Where, A is the sum of the areas of the adjacent faces around a vertex v_i. α_i and β_i denote the angle between two successive edges and dihedral angle of an edge respectively. Internal vertices of the mesh are ordered based on their curvature. Vertex with highest curvature is given the least priority and vertex with the least curvature is given the highest priority. This is to ensure that edges are eliminated in flat regions and edge collapsing in highly curved regions is delayed. After assigning priorities, vertices are maintained in a heap with least curvature vertex at the top.

- **Phase-II: Edge collapse**

The important features of the surface cannot be preserved by considering only the curvature of the vertex. This is because when the edge collapse takes place, adjacent triangles' shape is changed. Thus, the lowest priority vertex is eliminated by collapsing the edge ($e_{ij} \in \mathrm{E}_{v_i}$) that causes minimum geometric distortion in its local neighborhood. This edge is termed as optimal edge (e_o). For finding e_o, we employ a volume loss measure proposed by Lindstrom et al. [6] and also take into consideration the changes in shape of the adjacent triangles. An edge collapse e_{oi}: (v_o,v_i) -> v_i causes each triangle $t \in \mathrm{T}_{v_i}$ to sweep out a tetrahedral volume defined by the four vertices (v_i,v_1,v_2,v_o) as illustrated in Figure 5.

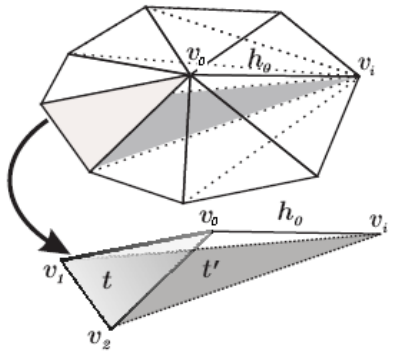

Figure 5. Volume Loss caused by Edge Collapse Operation [6]

The volume of this tetrahedron represents the volume loss due to the movement of t as a result of edge collapse and is indicative of the geometric deviation. The geometric deviation introduced due to triangle t (v_1, v_2, v_0) is defined in Equation (4).

$$V(t) = \frac{1}{6}\left[(v_1 - v_0) \times (v_2 - v_0).(v_1 - v_o)\right] \tag{4}$$

The geometric deviation introduced by the change in triangle shape is given as [15]:

$$S(t) = \frac{4\sqrt{3}A}{l_1^2 + l_2^2 + l_3^2} \tag{5}$$

Where l_1, l_2, l_3 are lengths of the edges and A is the area of the triangle. $S(t)$ takes values in the interval 0 to 1 indicating the equilateral triangle with 1 and the collinear triangle with 0. Finally, the total cost of collapsing an edge is given by:

$$Collapse\_Cost(e_{ij}) = \sum_{t \in T_{v_i}} V(t) * (1 - S(t)) \tag{6}$$

For each edge $e_{ij} \in E_{v_i}$, we compute *Collapse_Cost* (e_{ij}) and choose the one as optimal edge e_o for which *Collapse_Cost* (e_{ij}) is minimum. The proposed mesh simplification algorithm is summarized in Algorithm 2.

Algorithm 2: Mesh_Simplification
Input: Set *T* of triangles, *V* of vertices, *E* of edges and percentage of simplification P.
Output: Reduced set *T* of triangles, *V* of vertices and *E* of edges.

Begin

1. Calculate the curvature at each internal vertex using the following equation.

$$Curvature(v_i) = \sqrt{2H^2 - K}$$

   Where, *K* and *H* are Gaussian curvature and mean curvature at a vertex respectively. They are calculated using Equation (3).

2. Set curvature threshold to the average curvature at vertices.

$$Th = \frac{\sum_{i=1}^{n} Curvature(v_i)}{n}$$

3. Form candidate set of vertices based on curvature.
4. Insert all the candidate vertices into the heap with lowest curvature vertex at the top.
5. Perform edge collapse by selecting an optimal edge of the vertex.

   5.1. Remove top vertex from the heap.

   5.2. For each edge $e_{ij} \in E_{v_i}$, compute collapse cost using the following equation.

$$Collapse\_Cost(e_{ij}) = \sum_{t \in T_{v_i}} V(t) * (1 - S(t))$$

Where, $V(t)$ and $S(t)$ represent volume loss and triangle shape change which is incurred by collapsing edge e_{ij}. They are calculated using Equation (4) and Equation (5).

5.3. Select the optimal edge $e_o \in E_{v_i}$ such that

$$\text{Collapse\_Cost}(e_o) = \min\{\text{Collapse\_cost}(e_{ij}) | e_{ij} \in E_{v_i}\}$$

5.4. Collapse e_o : (v_i,v_j)->v_j, by eliminating faces incident on the edges $\{v_i,v_j\}$ and substituting v_j for every occurrence of v_i in the left over faces in T_{v_i}.

6. For each $v_i \in N_{v_i}$, compute its curvature and if it is less than the threshold then put it in candidate set and update heap.
7. Repeat steps 5 to 6 until the P% reduction of faces is achieved or the candidate set is empty.

End.

2.6. Rendering

In the final step, realistic effects are added to the surface of the 3D model by applying Phong lighting and shading model [16]. First the normals of the triangle vertices in the mesh are computed by taking the average of the adjacent triangle normals. Then the shading model linearly interpolates the vertex normal and then applies the lighting model at each point on the surface to determine the intensity at that point and thus shades the entire surface.

2.7. 3D Tumor Volume Computation

The volume of tumor is the vital information that can be extracted from the 3D model of tumor for knowing the severity of cancer and treatment planning. In this work, the volume of the tumor is estimated by considering the slice thickness, inter-slice gap and area of the tumor on each abnormal slice as given in the following equation.

$$Tumor\_volume = (Interslice\ \ gap + Slice\ \ thickness) * (\sum_{i=1}^{n} A_i) \quad (7)$$

Where, *n* indicates the total number of slices containing tumor and *A* is the area of tumor on each slice which is calculated by

$$A_i = No.\ of\ \ pixels\ \ in\ tumor\ region\ on\ slice\ \ i\ \ *\ \ Pixel\ \ dimension \quad (8)$$

3. Experimental Results

The proposed methods are implemented using MATLAB. All the experiments were performed on a personal computer with 3GHz Pentium processor and 3GB of memory running under Windows XP operating system.

3.1. Dataset

The input dataset consists of non enhanced T2-weighted brain MR images of 53 patients (female: 20, male: 33) with verified and untreated tumors. The patients' ages were in the range of 15 to 74 years (mean age: 48 years). Images were acquired from 1.5 Tesla MRI clinical scanner at Shirdi Sai Cancer Hospital, Manipal, India. The scan of each patient produced a set of slices with each slice having a thickness of 2mm and inter slice gap of 3mm. All images in the dataset were gray scale images with size 640x480. T2-weighted MR

images were used in the experiments as they provide appreciable contrast between brain regions.

3.2. Performance Evaluation

The performance of the proposed 3D reconstruction approach is evaluated in terms of effectiveness and efficiency.

3.2.1. Effectiveness of 3D reconstruction method: The proposed 3D reconstruction approach involves automatic segmentation of the brain tumor in non-contrast enhanced MR image. The MRI scan of the patient produces a set of slices containing normal and abnormal slices as shown in Figure 6. After identifying the abnormal slice, the tumor was segmented on that slice as shown in Figure 7.

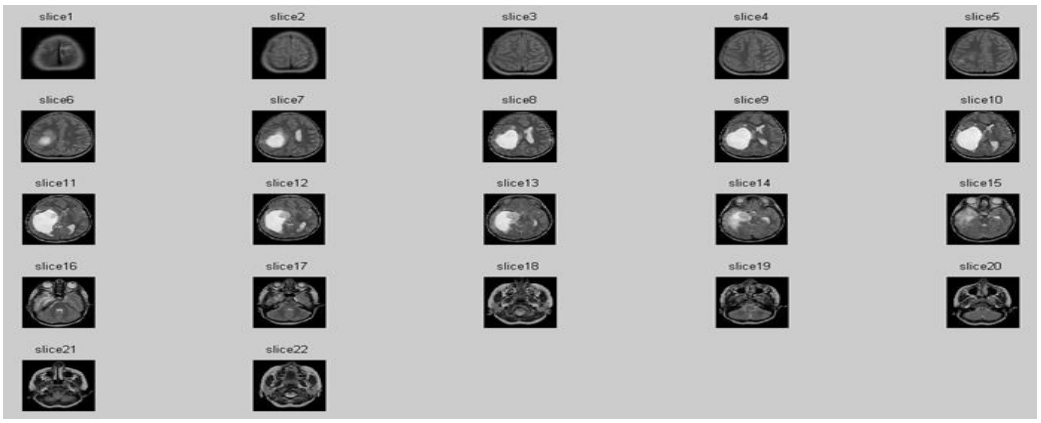

Figure 6. Set of Brain Slices

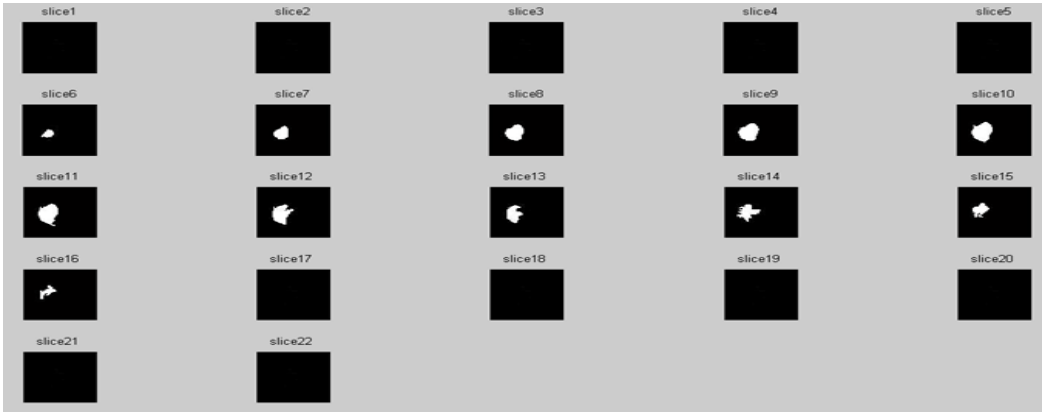

Figure 7. Set of Segmented Slices

The proposed segmentation technique was able to perfectly distinguish between normal and abnormal slices in a set of 1166 slices in the dataset as shown in Table 2.

Table 2. Slice Recognition Rate

Slice	Normal decision	Abnormal decision	Recognition rate
Normal slice	636/636	0/636	100%
Abnormal slice	0/530	530/530	100%

The evaluation of the segmentation results of the proposed method was performed through a quantitative comparison with the results of a manual segmentation carried out by an experienced radiologist. The quantitative comparison was made by calculating relative error which is given as follows:

$$\text{Relative error} = \frac{|N_p - N_g|}{N_g} \tag{9}$$

Where, N_p and N_g denote the total number of pixels in the segmented region generated by the proposed method and radiologist respectively. Table 3 shows the comparison between the automatic segmentation (proposed method) and the manual segmentation in terms of relative error of the segmented region. The average relative error computed over the entire dataset is 2.36%. This shows that the results of automatic segmentation provide a good match with the expert radiologist's results.

Table 3. Comparison of Automatic and Manual Segmentation Results

Case	Automatic segmentation (No. of Pixels in the tumor region)	Manual segmentation (No. of Pixels in the tumor region)	Relative Error (%)
1	1764	1805	2.27
2	3841	3785	1.47
3	1249	1231	1.46
4	2852	2793	2.11
5	3671	3755	2.23
6	4840	4783	1.19
7	1572	1581	0.56
8	2663	2735	2.63
9	4793	4631	3.49
10	3862	3828	0.88

After the tumor segmentation, 2D tumor contours are arranged exactly in real spatial positions. This forms the volume data of the tumor as shown in Figure 8 (a). We estimated the missing slices in the volume data by applying our proposed enhanced shape based interpolation technique on the sequential slices as shown in Figure 8 (b).

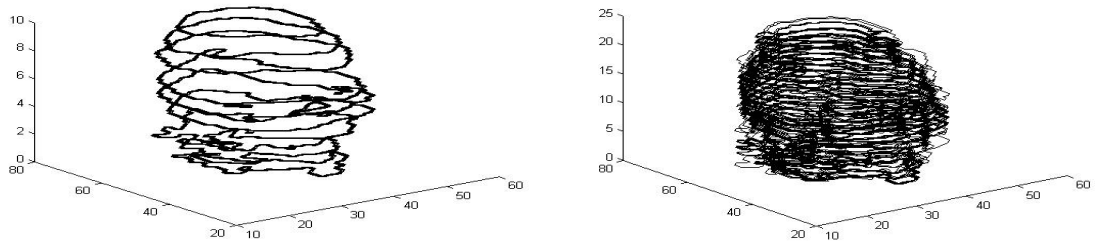

Figure 8. Stacking of Tumor Contours (a) Original Set of Contours (b) Set of Contours after Interpolation

In order to verify our enhanced shape based interpolation technique, we took three consecutive slices S_i, S_{i+1}, S_{i+2}. Slices S_i and S_{i+2} were considered as input to the proposed interpolation algorithm and slice $\hat{S}_{i+1}$ was estimated by the proposed method. The estimated slice was compared with the original slice S_{i+1} using the overlap-based error measure computed using Equation (10) as the ratio of the wrongly estimated pixels with respect to the area of the reference slice.

$$\varepsilon(S_{i+1}, \overset{\Lambda}{S}_{i+1}) = \frac{card(S_{i+1} \Delta \overset{\Lambda}{S}_{i+1})}{card(S_{i+1})} \tag{10}$$

Where, Δ is the symmetric difference and *card* is the cardinal function. This measure is computed for three interpolation methods: LG-linear gray level interpolation, SO-original shape based interpolation, SE: enhanced shape based interpolation (proposed method). The results are summarized in Table 4. It can be seen that proposed SE method outperforms other interpolation techniques as it takes into account shifts of a cross section in the slices.

Table 4. Comparison of Interpolation Results

Dataset	Slices (Si,Si+1,Si+2)	Error measure (ε %)		
		LG	SO	SE
MRI	4,5,6	6.91	5.22	5.03
	10,11,12	8.07	6.24	3.91
	18,19,20	11.17	8.79	3.33
	20,21,22	5.38	2.93	2.77

After the interpolation, surface mesh was reconstructed using the MC algorithm. In order to improve the rendering time and storage space, mesh was simplified using a proposed mesh simplification algorithm. We demonstrate the effectiveness of the proposed mesh simplification algorithm by presenting images of simplified models and error graphs. Figure 9 shows the simplified meshes and their corresponding rendered 3D models. In order to analyze the effectiveness, the original model was simplified at different levels (40%, 60%, 80%). It is

observed that even at 60% reduction the simplified model retains the features of the original model. The model gets distorted for reductions above 70%.

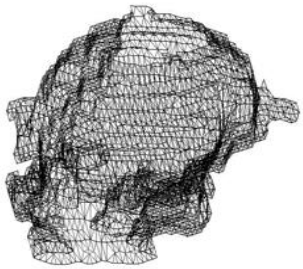

(a) Original mesh(P=0%, Faces=6116)

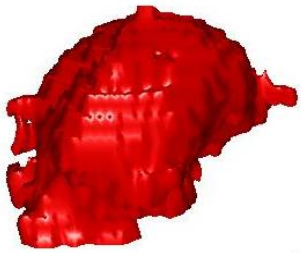

(e) Original 3D model(P=0%, Faces=6116)

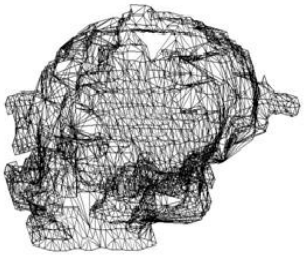

(b) Simplified mesh(P=40%, Faces=3669)

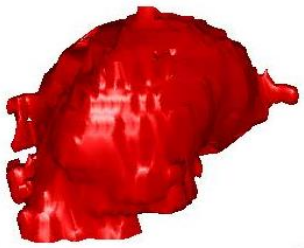

(f) Simplified 3D model(P=40%, Faces=3669)

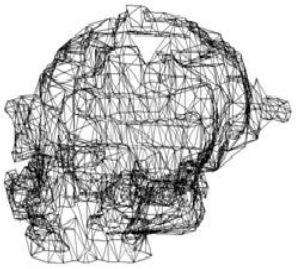

(c) Simplified mesh(P=60%, Faces=2446)

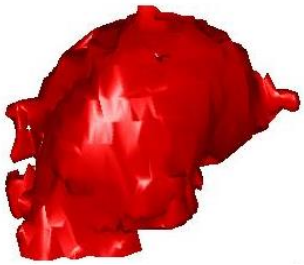

(g) Simplified 3D model(P=60%, Faces=2446)

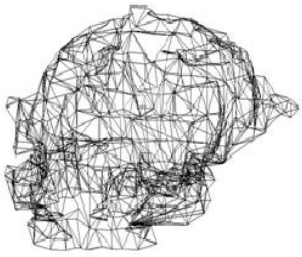

(d) Simplified mesh(P=80%, Faces=1223)

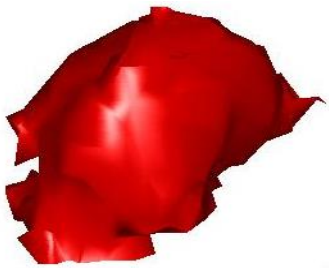

(h) Simplified 3D model(P=80%, Faces=1223)

Figure 9. Mesh Simplification Results

The quality of the simplified models is evaluated using symmetric Hausdorff distance (SHD). It measures the mesh approximation error by measuring the distance between the original and simplified mesh and is defined using the following equation.

$$SHD(M1, M2) = \max(\max_{v \in M1} d_v(M2), \max_{v \in M2} d_v(M1)) \quad (11)$$

Where, $d_v(M)$ is the minimum distance from vertex v to the closest vertex of mesh M. Figure 10 shows the comparison of the proposed method with other state of the art mesh simplification methods such as Qslim [5] and MS [6]. It can be seen that the proposed method has an improvement over Qslim and MS as it is based on selecting edge contractions with minimum effect on curvature, volume and shape of adjacent triangles. In order to assist the radiologist in staging of the brain tumor, the volume of the tumor is computed using Equation (7). The volume of the tumor shown in Figure 9 is computed as 215.26 mm^3.

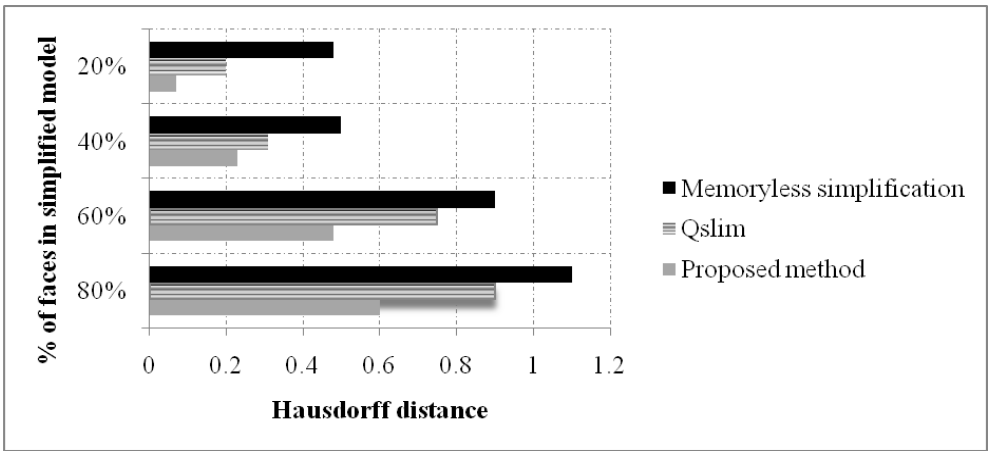

Figure 10. Comparison of Mesh Simplification Methods with SHD

We also provided the facility to rotate the reconstructed 3D model of the tumor so that the radiologist can analyze the structure of the tumor thoroughly. Two views of the 3D tumor are shown in Figure 11.

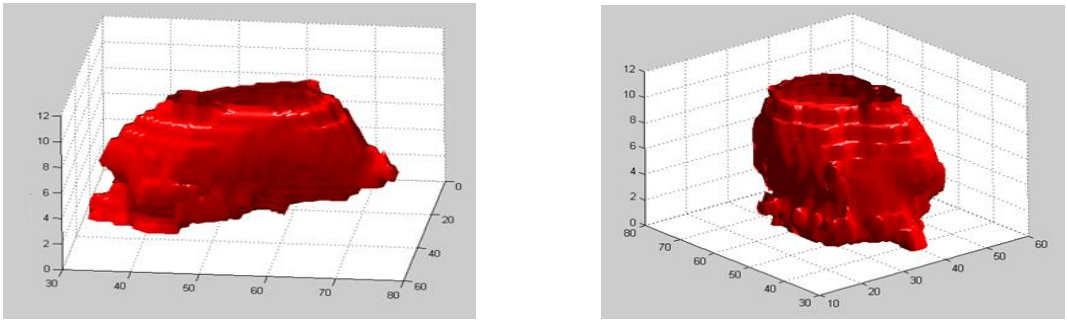

Figure 11. Two Views of the Tumor obtained by Rotation

The surface of the brain can also be reconstructed using the similar 3D reconstruction approach but by considering the brain region instead of tumor region. Using our proposed approach various types of cuts can also be performed on the brain by the radiologist in order to understand the tumor growth as shown in Figure 12.

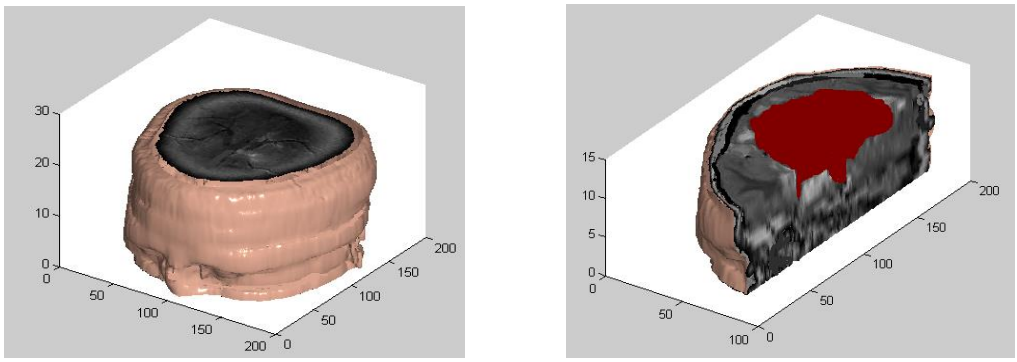

Figure 12. Cut away Surface (a) Traverse Cut (b) Longitudinal Cut

3.2.2. Efficiency of 3D reconstruction method: Table 5 shows the time complexity of different phases of 3D reconstruction of the brain tumor on MR images.

Table 5. Time Complexity of Different Phases of 3D Reconstruction of Tumor

3D reconstruction phase	Segmentation	Inter-Slice interpolation	Meshing	Mesh simplification	Rendering
Time complexity	*O(GCI)*	$O(N^2)$	*O(D)*	*O(VlogV)*	*O(T')*

Where, *G* is the number of gray levels in the image, *C* is the number of clusters, *I* is the number of iterations required for clustering algorithm to convergence, N is the total number of pixels in the image, *D* is the number of cubes processed in the reconstruction of the tumor, V is the number of vertices in the mesh, *T'* is the reduced set of triangles in the simplified mesh.

In the segmentation step of proposed 3D reconstruction approach, we make use of our previously proposed automatic brain tumor segmentation method which is based on MFCM clustering. It has a time complexity of *O(GCI)*. It takes less time to find the tumor cluster as it performs clustering on the basis of the gray level histogram of the image instead of pixels in the image. The number of gray levels is less than the number of pixels in the image. The proposed method SE takes less time for interpolation as it is based on the chamfer distance transform which computes the distance transform for each pixel using a local neighborhood. Thus, it results in time complexity of *O(N)*. The MC algorithm has time complexity *O(D)* to generate the 3D surface mesh of the tumor. The proposed mesh simplification method operates on the edges of a subset of vertices rather than on the entire vertices of the mesh. It makes one pass through the vertices to select the candidate vertices for edge collapse and then inserts them into a heap. It then performs maximum *V* pop operations where *V* is the total number of vertices, so its time complexity is *O(V log V)*. Whereas the time complexity of Qslim and MS algorithms is *O(E log E)*, where *E* is the total number of edges in the mesh. This is because in Qslim and MS algorithms, global greedy decision involves choosing an edge based on the error metric. Mesh simplification also accelerates the rendering time as the input to the rendering phase is the mesh with a reduced set of triangles *(T')* instead of a large number of triangles *(T)* generated by the MC algorithm.

4. Conclusion

The aim of this paper was to develop a 3D reconstruction and quantification approach for assisting the physician in surgical planning and volume computation of the tumor. The 3D model of the brain tumor was reconstructed from a given set of 2D slices of the brain by developing methods for segmentation, inter-slice interpolation, mesh generation and simplification. Slices containing tumor were extracted from a given set of slices of the brain and the tumor was segmented with the proposed segmentation technique. The centroid alignment technique in the proposed enhanced shape based interpolation helped in accurately estimating the missing slices by handling the shifts in the cross sections and the inclusion of the chamfer distance transform improved the efficiency of shape based interpolation method. Rendering phase was accelerated by simplifying the mesh with the proposed mesh simplification algorithm. The reconstructed tumor was also quantified by measuring its volume. The experimental results showed that our proposed 3D reconstruction approach can generate an accurate 3D model in less amount of time and thus can assist the radiologist in the diagnosis, identifying the stage of the tumor and treatment planning.

References

[1] K. Narayan and Y. Karunakar, "3-D Reconstruction of Tumors in MRI Images", International Journal of Research and Reviews in Signal Acquisition and Processing, vol. 2, no. 1, **(2011)**.
[2] N. Archip, R. Rohling, V. Dessenne, P. J. Erard and L. P. Nolte, "Anatomical structure modeling from medical images", Computer Methods and Programs in Biomedicine, vol. 82, **(2006)**.
[3] S. P. Raya and J. K. Udupa, "Shape based interpolation of multidimensional objects", IEEE Transaction on Medical Imaging, vol. 1, no. 9, **(1990)**.
[4] W. E. Lorensen and H. E. Cline, "Marching cubes: a high resolution 3-D surface construction algorithm", Computer Graphics, vol. 4, no. 21, **(1987)**.
[5] M. Garland and P. S. Heckbert, "Surface simplification using quadric error metrics", SIGGRAPH '97 Proceedings of the 24th annual conference on Computer graphics and interactive techniques, **(1997)**.
[6] P. Lindstrom and G. Turk, "Fast and memory efficient polygonal simplification", Proceedings of Conference on Visualization, **(1998)**.
[7] A. Castro, C. Bveda and B. Arcay, "A new method for the initialization of clustering algorithms based on histogram analysis", IASTED International Conference on Visualization, Imaging and Image Processing, ACM, **(2007)**.
[8] M. P. Arakeri and G. R. M. Reddy, "Efficient fuzzy clustering based approach to brain tumor segmentation on MR images", Proceedings of CIIT 2011, CCIS. Springer, vol. vol. 250, **(2011)**.
[9] P. E. Danielsson, "Euclidian distance mapping", Computer Graphics and Image Processing, vol. 14, **(1980)**.
[10] G. T. Herman, J. Zheng and C. A. Bucholtz, "Shape-based interpolation", IEEE Computer Graphics and Applications, vol. 3, no. 12, **(1992)**.
[11] G. Borgefors, "Distance transformations in digital images", Computer Vision, Graphics and Image Processing, vol. 34, **(1986)**.
[12] M. J. Durst, "Additional reference to marching cubes", Computer Graphics, vol. 4, no. 22, **(1988)**.
[13] C. Montani, R. Scateni and R. Scopigno, "A modified look-up table for implicit disambiguation of marching cubes", The Visual Computer, vol. 10, **(1994)**.
[14] N. Dyn, K. Hormann, S. J. Kim and D. Levin, "Optimizing 3D triangulations using discrete curvature analysis", Mathematical Methods for Curves and Surfaces, **(2001)**.
[15] L. Wang, J. Li and I. Hagiwara, "A topology preserved mesh simplification algorithm", World Congress on Computer Science and Information Engineering, **(2009)**.
[16] J. D. Foley, A. Van Dam, S. K.. Feiner and J. F. Hughes, "Computer graphics: principles and practice", 2nd Edition, Addison-Wesley, **(1997)**.

Authors

Megha P. Arakeri, obtained her masters degree in computer science from Jawaharlal Nehru National College of Engineering, Shimoga, India. She is currently pursuing Ph.D in Medical Image Processing at National Institute of Technology Karnataka, Surathkal, India. Her research interests include Medical Image Processing, Computer Vision, Information Retrieval and Pattern Recognition.

G. Ram Mohana Reddy, he is a Professor in Information Technology Department, National Institute of Technology Karnataka, Surathkal, India. He received his masters degree from Indian Institute of Technology, Kharagpur, India. He was awarded common wealth fellowship for pursuing Doctoral Research at University of Edinburgh, U.K. His research interests include Applied Perception, Human Computer Interaction and High Performance Computing.